

30-MHz Power Inductor Using Nano-Granular Magnetic Material

Shanshan Lu
Yuqin Sun
M. Goldbeck
D. R. Zimmanck
C. R. Sullivan

Found in *IEEE Power Electronics Specialists Conference*, June 2007,
pp. 1773–1776.

©2007 IEEE. Personal use of this material is permitted. However, permission to reprint or republish this material for advertising or promotional purposes or for creating new collective works for resale or redistribution to servers or lists, or to reuse any copyrighted component of this work in other works must be obtained from the IEEE.

30-MHz Power Inductor Using Nano-Granular Magnetic Material

Shanshan Lu, Yuqin Sun, Marissa Goldbeck, Donald R. Zimmanck, Charles R. Sullivan
Thayer School of Engineering at Dartmouth, Hanover, NH 03755,
http://power.thayer.dartmouth.edu shanshan.lu@dartmouth.edu

Abstract—Nano-granular metal-nonmetal soft magnetic materials offer low losses at frequencies up to 100 MHz, with higher flux density and temperature capability than ferrites. We present the design, fabrication, and testing of a high- Q 30 MHz toroidal inductor using Co-Zr-O nano-granular magnetic materials.

I. INTRODUCTION

Nano-granular metal-nonmetal soft magnetic materials consist of nano-grains of a magnetic metal in a ceramic matrix [1]–[8]. The ceramic leads to high overall resistivity, while the metal grains are too small for significant eddy currents to circulate within them, typically 2 to 10 nm. Thin films of these materials can have anisotropic behavior that leads to low hysteresis losses. The losses can be low up to on the order of 100 MHz, with higher flux density and temperature capability than ferrites. Some of their characteristics are similar to nanocrystalline materials, but the ceramic leads to much higher resistivity and thus much higher frequency capability [8].

The particle size below 10 nm is much smaller than is necessary to reduce inter-particle eddy currents to negligible levels. However, for particles in the nm size range, coercivity tends to increase with increasing particle size, and so low hysteresis losses are easier to achieve with small particles. This is contrary to the trend for μm size particles, where larger particles have lower coercivity. The different trend is due to the particles being small compared to the size of a magnetic domain [9].

Most nano-granular materials are deposited by a reactive sputtering thin-film deposition process, which typically produces films a few microns thick, though we have produced good quality films as thick as $10\ \mu\text{m}$ [10]. Thus, typical applications have been to microfabricated inductors, for example on Si substrates [11], [12], [13], typically with very low inductance values, for low-impedance applications. In order to achieve higher inductance values and high Q values, we stack multiple polyimide substrates to build up a larger total thickness of magnetic material and to form a toroidal core, similar to the approach in [14]. We then deposit a thin layer of copper which is etched to form a 12-turn winding around the toroid. In this paper, we report the design, fabrication, and testing of such an inductor, intended to be applied as a resonant inductor in a 30 MHz 100 W power converter [15][16][17].

Although completing a careful design before fabrication is of the possibilities allowed by the fabrication process. Thus we

start by discussing the fabrication process before detailing the design optimization.

II. FABRICATION

We constructed a core for an inductor by stacking multiple $50\ \mu\text{m}$ polyimide substrates, each with $6\ \mu\text{m}$ of Co-Zr-O granular magnetic material sputtered on each side. The result is a sheet $62\ \mu\text{m}$ thick, of which 20% is magnetic material.

The magnetic material is anisotropic, and only has low hysteresis loss for flux travelling in one direction in the

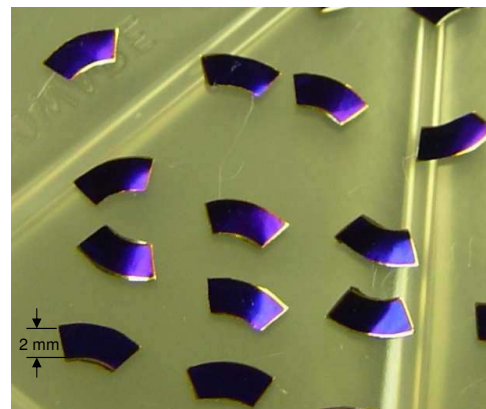


Fig. 1. Segments of magnetic material deposited on thin polyimide substrates.

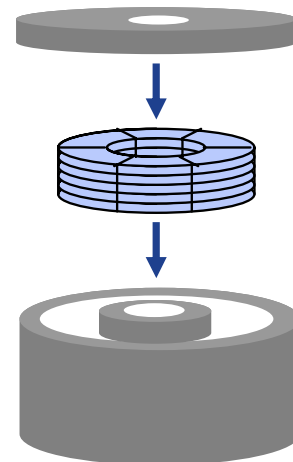


Fig. 2. Schematic of core fabrication. Stacked segments of core material are assembled into a high-temperature polymer toroidal box.

plane—the “hard axis” direction [18]. To construct a closed core, it is necessary to either bend the substrates or connect multiple substrates, each with a different orientation of the hard axis. We construct a toroidal core from six segments, as shown in Fig. 2. This also allows adding gaps between each segment to construct a “quasi-distributed” gap [19]. Each segment consists of 40 stacked substrates, which are then assembled into a toroidal box made of Ensinger Tecamida (a high-temperature polymer which can stand up to 262 °C), as shown in Fig. 2. On top of the box, a lid is then glued as shown in Fig. 3. We also drilled a hole with a diameter of 1 mm on the side wall of the box to keep the pressure from building up inside since an entirely closed box may explode in the vacuum environment during the copper sputtering process.

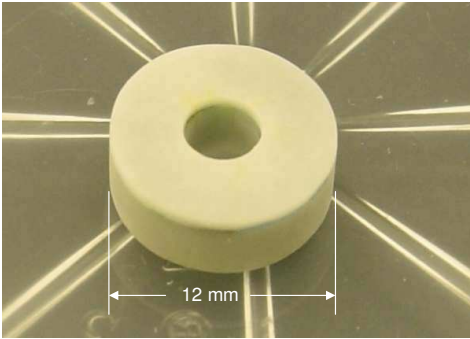


Fig. 3. Completed core in a high-temperature polymer box.

To form a coil around this core, we deposited copper over the whole surface by performing several sputter depositions. We then electroplated thicker copper, for about 20 to 30 μm total copper thickness. To define individual turns, we masked the copper and etched lines between the turns. The mask for such a process would ordinarily be patterned by photolithography, but this is difficult on a three-dimensional surface, so we instead opened slits in the masking layer with a scalpel blade moved across the surface with a micropositioning system, maintaining light contact with the copper through monitoring contact resistance.

The completed inductor coil on the stacked core is shown in Fig. 4. Since the etch process was not well controlled, the etched lines between turns are larger than we desired. Thus, we developed a new process using sharpened scroll saw and circular saw blades to make finer cuts. The details of this process are described in [20].

III. DESIGN

The specific geometrical parameters of the design were chosen through the use of a numerical optimization using a performance calculation program written specifically for these inductors. The design was constrained to have significant gap reluctance in order to make the inductance robust against possible variations in permeability of the core due to temperature or process variations.

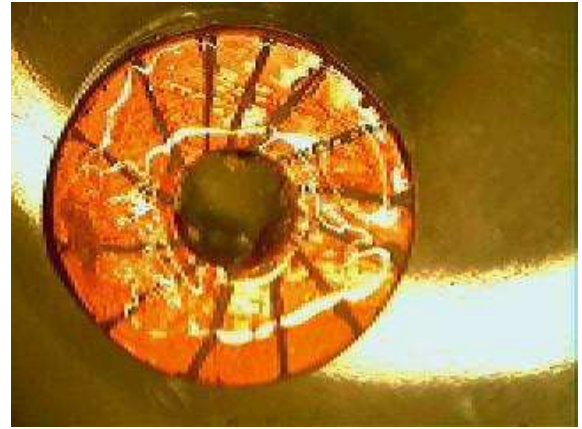


Fig. 4. Patterned winding on stacked nano-granular core.

Losses in the core were calculated based on eddy currents within each layer of magnetic material. Hysteresis losses are expected to be small based on the nearly ideal behavior found in the anisotropic material with excitation in the hard-axis direction; although small coercivity appears in some samples when the sample is driven all the way to saturation in both directions, the loop closes up when it kept out of saturation. Nonetheless, we conservatively assume non-zero hysteresis loss. Inductance was calculated including the flux in the magnetic material, the flux in the stacked substrates, and the flux in the walls of the box. Although the flux densities in the polymer materials are much lower than in the magnetic material, the total flux in non-magnetic materials is significant since the magnetic material is only 20% of the thickness of the stacked of magnetic material and substrates. The winding loss is calculated using the approximate formula in [19] to estimate the effect of the fringing fields from the multiple gaps on the ac resistance. We write ac resistance as

$$R_{ac} = F_g R_\delta \quad (1)$$

where R_δ is the resistance of a layer one skin-depth thick (the ac resistance without any gap fringing effect) and F_g is a factor accounting for the gap effect, approximated by

$$F_g(s, p) = \frac{1}{2} \cdot \left[\frac{-k}{(b^{-n} + p^{-n})^{1/n}} + k \cdot p + 1.9 \right] \quad (2)$$

where n , k , and b are curve fitting constants from [19]:

$$n = 5.4 \quad (3)$$

$$k = \frac{0.95}{0.95 + 1.4 \cdot s} \quad (4)$$

$$b = 3.33 \cdot s + 2.14 \quad (5)$$

where s is the spacing of the conductor away from the core and p is the gap pitch (distance between gaps).

TABLE I
INDUCTOR DESIGN

Material and Performance Specifications
(input to design calculations)

Application Requirements	
Frequency	30 MHz
AC current through the inductor	3.8 A rms
Inductance	325 nH
Magnetic material properties	
Maximum flux density	1 T
Permeability	$80\mu_0$

Design Details

* indicates values that may be significantly different in the fabricated inductor.

Core	
Magnetic material thickness	6 μm on each side of each substrate
Substrate thickness	50 μm
Number of substrates per segment	40
Gap between each segment	190 μm *
Core box (coil former)	
Outside diameter	12 mm
Inside diameter (center hole)	4 mm
Overall height	4.1 mm
Wall thickness	0.5 mm
Coil	
Number of turns	12
Copper thickness	17.4 μm *
Slit width between turns	50 μm *

Predicted Performance

Q	148
AC winding loss	4.91 W
Hysteresis loss	1.12 W
Eddy current loss	0.0016 W

The Q of this inductor was calculated based on an equivalent circuit consisting of a series LR circuit in parallel with a capacitor C . It contains 1) the inductance L ; 2) resistors R_w , R_h , and R_e in series representing ac winding loss, hysteresis loss and eddy current loss, respectively; and 3) a capacitor C representing the total effective capacitance including that between adjacent turns, top and bottom sections of a single turn, in addition to the inner and outer sections of a single turn. The Q was calculated as the ratio of the imaginary part of the impedance of this network to the real part of its impedance.

The design chosen and its performance calculated from the equivalent circuit are shown in Table I.

The design is intended for a resonant application in which the ac current is higher than the dc current. The dc resistance can easily be made much smaller than the ac resistance simply by increasing the copper thickness; for example, 50 μm copper leads to dc resistance one fifth of the ac resistance. However, for applications with large dc current and small to moderate ac resistance, high Q is less important and simpler designs (e.g. [12]) may be preferred.

IV. EXPERIMENTAL RESULTS

The design described in Section III was fabricated following the process described in Section II. The final inductor does not match the design precisely. Most importantly, the gaps were fabricated using 100 μm spacer sheets, with the expectation that imperfect packing would lead to larger gaps. The measured inductance of 470 nH shows that slightly thicker spacers would be needed to achieve the 325 nH design value of inductance. In addition, the etching process was not as well controlled in the actual fabrication as it had been on test pieces, leading to wide and variable spacing between turns, on the order of 200 μm , much greater than the 50 μm design value.

A precision impedance analyzer (Agilent 4294A) was used to measure the completed inductor's impedance, using a low-residual-impedance test fixture [21] to connect the inductor. Because the inductor has high Q , small phase errors can result in large errors in the measured loss [21]. To get around this problem, the inductor was measured in series with a high- Q mica capacitor. Various capacitor values were used for resonances in the range of 20 to 40 MHz. Near the resonance frequency, the capacitor cancels most of the inductor's reactance, such that the inductor ESR is a much larger fraction of the total measured impedance. This makes the ESR measurement much less sensitive to small phase errors.

From the ESR obtained from this measurement and inductance measured directly, Q was calculated, and is plotted in Fig. 5. At the design frequency, Q is 67, and remains close to that value throughout the measured range. This is 45% of the predicted Q of 148. We attribute the difference primarily to imperfections in the coil fabrication in this sample, and we expect to achieve closer to the design value in future samples.

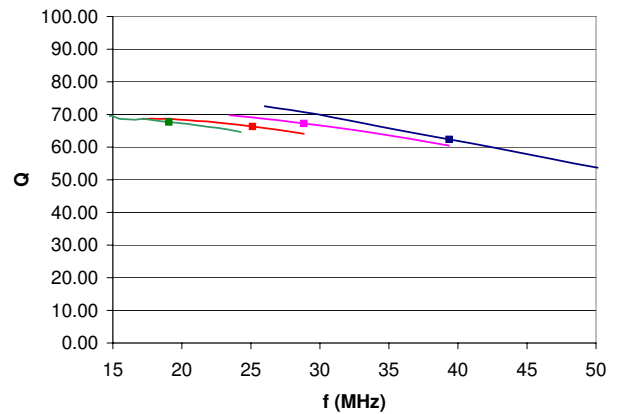


Fig. 5. Plot of measured inductor Q as a function of frequency. Each curve is obtained from ESR measured with a different series capacitor, and is most accurate near the resonance point, marked with ■.

V. CONCLUSION

Nano-granular metal-nonmetal soft magnetic materials offer attractive properties for applications in the range of tens of

MHz. A 30 MHz toroidal inductor using Co-Zr-O nanogranular magnetic materials has been designed, fabricated and tested. A 12 mm diameter, 4.1 mm high inductor achieves an inductance of 470 nH with a Q of 67. Process improvements underway should allow nearly doubling this Q value.

REFERENCES

- [1] P. Dhagat, S. Prabhakaran, and C. Sullivan, "Comparison of magnetic materials for V-groove inductors and mosfets in optimised high-frequency dc-dc converters," *IEEE Transactions on Magnetics*, vol. 40, no. 4, pp. 2008–2010, 2004.
- [2] S. Ohnuma, H. Fujimori, S. Furukawa, S. Mitani, and T. Masumoto, "Co-(N, O)-based granular thin films and their soft magnetic properties," *Journal of Alloys and Compounds*, vol. 222, pp. 167–172, 1995.
- [3] H. Fujimori, "Structure and 100 MHz soft magnetic properties in multilayers and granular thin films," *Scripta Metallurgica et Materialia*, vol. 33, no. 10/11, pp. 1625–1636, 1995.
- [4] Y. Hayakawa and A. Makino, "Soft magnetic properties of Fe-M-O (M=Hf, Zr, Y, Ce) films with high electrical resistivity," *NanoStructured Materials*, vol. 6, pp. 989–992, 1995.
- [5] S. Ohnuma, H. Fujimori, S. Mitani, and T. Masumoto, "High-frequency magnetic properties in metal-nonmetal granular films," *Journal of Applied Physics*, vol. 79, no. 8, pp. 5130–5135, April 1996.
- [6] S. Ohnuma, H. J. Lee, N. Kobayashi, H. Fujimori, and T. Masumoto, "Co-Zr-O Nano-Granular Thin Films with Improved High Frequency Soft Magnetic Properties," *IEEE Transactions on Magnetics*, vol. 37, no. 4, pp. 3759–3761, July 2001.
- [7] Y. Sun, W. Li, P. Dhagat, and C. R. Sullivan, "Perpendicular anisotropy in granular Co-Zr-O films," *Journal of Applied Physics*, vol. 97, no. 10, p. 10N301, 2005.
- [8] W. Li, Y. Sun, and C. Sullivan, "High-frequency resistivity of soft magnetic granular films," *IEEE Transactions on Magnetics*, vol. 41, no. 10, pp. 3283–3285, 2005.
- [9] B. D. Cullity, *Introduction to magnetic materials*. Addison-Welsey, 1972.
- [10] C. R. Sullivan, S. Prabhakaran, P. Dhagat, and Y. Sun, "Thin-film inductor designs and materials for high-current low-voltage power," *Transactions of the Magnetics Society of Japan*, vol. 3, no. 4, pp. 126–8, 2003.
- [11] S. Prabhakaran, C. Sullivan, and K. Venkatachalam, "Measured Electrical Performance of V-Groove Inductors for Microprocessor Power Delivery," *IEEE Transactions on Magnetics*, vol. 39, no. 5, pp. 3190 – 3192, 2003.
- [12] S. Prabhakaran, Y. Sun, P. Dhagat, W. dong Li, and C. R. Sullivan, "Microfabricated V-Groove Power Inductors for High-Current Low-Voltage Fast-Transient DC-DC Converters," in *36th Annual IEEE Power Electronics Specialists Conference.*, 2005.
- [13] Y. Sasaki, S. Morita, T. Hatanai, A. Makino, T. Sato, and K. Yamasawa, "Application of nanocrystalline Fe(or Co-Fe)-Hf-O magnetic films with high electrical resistivity to micro DC-DC converters," *NanoStructured Materials*, vol. 8, no. 8, pp. 1025–1032, 1997.
- [14] K. Takei, O. Ishii, and M. Senda, "Application of magnetic metal thin films to em1 noise filter," in *IEEE International Symposium on Electromagnetic Compatibility*, 1996, pp. 508 – 510.
- [15] J. M. Rivas, D. Jackson, O. Leitermann, A. D. Sagneri, Y. Han, and D. J. Perreault, "Design considerations for very high frequency dc-dc converters," in *37th IEEE Power Electronics Specialists Conference*, 2006.
- [16] J. M. Rivas, Y. Han, O. Leitermann, A. Sagneri, and D. Perreault, "A high-frequency resonant inverter topology with low voltage stress," in *38th IEEE Power Electronics Specialists Conference*, 2007.
- [17] R. Pilawa-Podgurski, A. Sagneri, J. Rivas, D. Anderson, and D. Perreault, "Very high frequency resonant boost converters," in *38th IEEE Power Electronics Specialists Conference*, 2007.
- [18] C. R. Sullivan and S. R. Sanders, "Design of microfabricated transformers and inductors for high-frequency power conversion," *IEEE Trans. on Power Electronics*, vol. 11, no. 2, pp. 228–238, 1996.
- [19] J. Hu and C. R. Sullivan, "AC resistance of planar power inductors and the quasi-distributed gap technique," *IEEE Transactions on Power Electronics*, vol. 16, no. 4, pp. 558–567, 2001.
- [20] C. R. Sullivan, W. Li, S. Prabhakaran, and S. Lu, "Design and fabrication of low-loss toroidal air-core inductors," in *38th IEEE Power Electronics Specialists Conference*, 2007.
- [21] S. Prabhakaran and C. R. Sullivan, "Impedance-Analyzer Measurements of High Frequency Power Passives: Techniques for High Power and Low Impedance," in *IEEE Industry Applications Society Annual Meeting*, Oct. 2002.